International Food Research Journal 31(3): 770 - 783 (June 2024)
Journal homepage: *http://www.ifrj.upm.edu.my*

Effect of polyphenols from kiwi by-products (PKWP) on redox and metabolic homeostasis of HepG2 cells

[1]*Wang, J., [1]Jin, D. L., [1]Fang, L. L., [1]Yu, J. F., [2]Wang, M., [1]Yang, W. J., [1]Yao, W. B., [1]*Wang, J. K., [1]Li, N. and [1]Gong, P.

[1]*School of Food Science and Engineering, Shaanxi University of Science and Technology, Xi'an 710021, China*
[2]*Nanyuan Hospital, Beijing 100076, China*

Article history

Received:
26 January 2024
Received in revised form:
22 April 2024
Accepted:
26 April 2024

Keywords

anti-cancer activity,
metabolism,
oxidative stress,
PKWP,
polyphenols

Abstract

Polyphenols from kiwi by-products (PKWP) have been previously reported to have an inhibitory effect on cancer cells; but, the potential anti-cancer mechanism remains unknown. Metabolic alterations in cancer cells provide bioenergy and substances for uncontrolled proliferation and development, and interfering with the metabolic pathways has been regarded as effective in impeding cancer progression. Cancer cells are also characterised by a relatively higher level of oxidative stress and an enhanced antioxidant defence system, facilitating multiple stages of tumorigenesis. Anti-cancer mechanisms of PKWP based on metabolic and redox homeostasis in HepG2 cells were thus investigated in the present work. The results showed that PKWP effectively decreased HepG2 cell viability in a concentration-dependent manner. PKWP caused metabolic disorders in HepG2 cells, and significantly affected the content of about 32 metabolites. PKWP mainly inhibited saccharide synthesis and glycolysis, and restricted the utilisation of amino acids. PKWP stimulated ROS production, and caused lipid peroxidation, resulting in oxidative damage. PKWP also down-regulated the activities of T-SOD and CAT, and the level of GSH, and inhibited the protein expressions of HO-1 and COX-2, weakening the cellular antioxidant capacity. Thus, PKWP could exert prominent anti-cancer activity in HepG2 cells by disrupting metabolic homeostasis, and induction of oxidative stress. These findings will provide evidence for further elucidation of the anti-cancer mechanism of PKWP, and the potential application of PKWP as a natural ingredient in functional food, cosmetic, and pharmaceutical industries.

DOI
https://doi.org/10.47836/ifrj.31.3.20

Introduction

Dietary polyphenols are commonly found in peels, leaves, pulp, and roots of plants. Fruits and vegetables are important sources of these polyphenol compounds. Polyphenols of plant origin have various biological functions such as anti-cancer, anti-inflammatory, and obesity prevention activities (Li *et al*., 2023). Therefore, polyphenols can be used for health-promoting functional foods (Çam *et al*., 2014; Chen *et al*., 2022).

Kiwi is the best-known fruit of family Actinidiaceae that has become a popular product around the world due to its nutritional values and versatile health benefits (Wang *et al*., 2021). Although kiwi is usually consumed fresh, it is also used to produce juices, wines, jams, *etc*. This industrialisation yields kiwi by-products, especially peels, seeds, and discards. These by-products have attracted interest as they are rich sources of bioactive compounds such as triterpenes, carotenoids, and polyphenols (Sanz *et al*., 2021). Moreover, it has also been found that the content of polyphenols in the peel residue of kiwi is higher than that in the pulp (Dias *et al*., 2020; Echave *et al*., 2021). Therefore, kiwi by-products represent a valuable source of phenolic compounds. It was reported that polyphenols from kiwi by-products (PKWP) could suppress the proliferation of cancer cells such as MCF7, NCI H460, HeLa, and HepG2 (Alim *et al*., 2019; Dias *et al*., 2020), indicating a strong potential of anti-cancer activity. However, the underlying anti-cancer mechanisms of PKWP have not been elucidated in previous studies.

*Corresponding author.
Email: wangjingsp@sust.edu.cn ; rjiankangwang@outlook.com

The homeostasis among the catabolic pathways, anabolic pathways, and waste disposal are essential for cell survival, growth, differentiation, and death. The metabolic requirements of proliferating cells differ from those of non-proliferating cells due to the substantial energy demand for over-proliferating cells. Cancer cells characterised by over-proliferation maintain metabolic homeostasis to grow and survive in hostile microenvironments by metabolic reprogramming. Metabolic reprogramming is a crucial cancer hallmark, which satisfies a large amount of energy demand, maintains redox homeostasis, and generates the building blocks, as well as produces numerous key signalling metabolites for the massive proliferation, differentiation, and survival (Finley, 2023). Metabolic reprogramming also plays a vital role in cancer malignancies and therapy resistance. Thus, targeting the abnormal metabolism of cancer cells is likely to inhibit cancerous cell proliferation, which provides potential prospects for cancer treatment (Kroemer and Pouyssegur, 2008).

Metabolomics, an emerging approach, explores the metabolic characteristics of endogenous small-molecule metabolites (molecular weight of less than 1,000) during physiological or pathological conditions. Metabolomics allows the metabolome to collect more information about the changes in metabolites, and is more dynamic than the genome and transcriptome (Li *et al*., 2022; Pang and Hu, 2023). It is of great value for the characteristics research of cancer metabolism using metabolomics.

The metabolic shift, such as a glycolytic shift in cancer cells, contributes to the alteration in redox (oxidation-reduction reaction) states (Tuy *et al*., 2021). The dynamic regulation of intracellular redox status is closely related to cell growth, proliferation, and senescence. Redox balance is essential for human health as its disturbance could lead to acute and chronic diseases, including atherosclerosis, type 2 diabetes, obstructive pulmonary disease, Alzheimer's disease, as well as cancers. Redox imbalance leads to oxidant burden, and is generally defined as oxidative stress (OS). Oxidative stress occurs readily when the body cannot counteract or detoxify pro-oxidant substances, such as reactive oxygen species (ROS) generated within the body (Rotariu *et al*., 2022). ROS are natural products typically generated by the metabolism of various substances and the energy production of mitochondria (Lennicke and Cochemé, 2021). Due to the frequent occurrence of ROS in cancer cells, cancer cells require multiple mechanisms for controlling or mitigating OS to promote malignant behaviour. ROS have already become an emerging hallmark of cancers (Zhou *et al*., 2023). However, restoring the antioxidant activity in cancer cells fails to effectively suppress cancer initiation and progression. Surprisingly, studies have found that most bioactive substances and nanoparticles such as Baicalin, Shikonin, and pomegranate polyphenols could induce cancer cell death by directly or indirectly facilitating the accumulation of ROS (Sanati *et al*., 2022; Yuan *et al*., 2023; Qian *et al*., 2023; Mukherjee *et al*., 2023). This is because cancer cells are more sensitive to ROS. Triggering cytotoxic ROS in cancer cells can be promising for controlling the growth of cancer cells. Oxidative stress-mediated cell death has already been considered a common anti-cancer mechanism for several substances bearing anti-cancer bioactivity (Jiang *et al*., 2023).

Hepatocellular carcinoma (HCC) is a global leading cause of cancer-related death, with a high incidence and mortality rate. There are many causes for HCC, such as exposure to toxins, HCV infection, alcohol abuse, and non-alcoholic fatty liver disease, apart from genetic factors. Although research on cancers has achieved significant progress, HCC still lacks effective early diagnosis, as well as better treatments. Thus, patients suffering from HCC are accompanied by a high 5-year recurrence rate of nearly 70% (Zhong *et al*., 2023). It is predicted that the number of new cases of liver cancer is likely to increase by 55.0% between 2020 and 2040, with about 1.4 million new diagnoses forecast for 2040 (Rumgay *et al*., 2022). Thus, the burden of HCC is heavy, and still a principal health issue in the world. HepG2 is a human hepatocyte carcinoma cell line derived from a well-differentiated human hepatoblastoma, and is widely used as an *in vitro* model for liver cancer research. As PKWP has been reported to suppress the growth of HepG2 cancer cells (Alim *et al*., 2019; Dias *et al*., 2020); in the present work, the effect of PKWP on the metabolism of HepG2 cells was investigated using the metabolomics approach, and the redox status was also studied to elucidate the underlying anti-cancer mechanism. The present work may provide a reference for the in-depth research and potential application of PKWP in the near future.

Materials and methods

Chemicals and reagents

DMEM medium was purchased from Gibco (Invitrogen Corporation, USA). Foetal bovine serum (EVERY GREEN) was provided by Tianhang Biotechnology (Zhejiang, China). MTT (3-(4,5-Dimethyl-2-thiazolyl)-2,5-diphenyl-2H-tetrazolium bromide), dimethyl sulfoxide (DMSO), methylamine hydrochloride, N-Methyl-N-(trimethylsilyl)trifluoroacetamide (MSTFA), and tridecanoic acid were purchased from Sigma-Aldrich (USA). The assay kits for malondialdehyde (MDA), total superoxide dismutase (T-SOD), catalase (CAT), and bicinchoninic acid (BCA) for protein determination were provided by the Beyotime Institute of Biotechnology (Jiangsu, China). Penicillin-Streptomycin Liquid (100×) and Trypsin-EDTA solution were purchased from Solarbio Life Science (Beijing, China). Polyvinylidene fluoride (PVDF) was from Millipore (USA). GAPDH (sc-365062), Heme Oxygenase 1 (HO-1, sc-136960), and Cyclooxygenase-2 (COX-2, sc-376861) were obtained from Santa Cruz Biotechnology (California, CA, USA). Western Blotting Detection Reagents were obtained from Engreen Biosystem (Beijing, China). RIPA Lysis Buffer and DCFH-DA (2',7'-Dichlorodihydrofluorescein diacetate) and Peroxidase-Conjugated AffiniPure Goat Anti-Mouse IgG were obtained from Beyotime Institute of Biotechnology (Jiangsu, China). The assay kit of glutathione (GSH) was from Bioss Antibodies (Beijing, China). All other reagents were commercial products of the highest available purity grade.

PKWP extraction and purification

The peel residue of Xu Xiang kiwifruit was collected, dried, and crushed. The peel residue powder was stored in a cool place for later use. About 10 g of kiwifruit peel residue powder was mixed with 250 mL of ethanol solution (60%) and cellulase (0.2%, w/v). After enzymatic hydrolysis at 55°C for 60 min, the enzyme was inactivated in boiling water. The mixture was allowed for extraction at 70°C for 150 min, and the crude extract of PKWP was obtained by filtration. The crude extract was mixed with the macro-porous adsorption resin at a ratio of 0.04 (w/v). After shaking at 120 rpm at 30°C for 24 h, the resin was cleaned with distilled water, and then ethanol solution (60%) was added to the eluent by shaking (120 rpm) at 30°C for 24 h. The eluent was evaporated and lyophilised to obtain purified PKWP, and stored in a refrigerator at 4°C for later use.

Cell culture

Human hepatocellular carcinoma HepG2 cells were purchased from the Cell Bank of the Chinese Academy of Sciences (Shaanxi, China). HepG2 cells were cultured in DMEM medium supplemented with 10% foetal bovine serum (FBS) and 1% penicillin-streptomycin liquid (100×) at 37°C and in an atmosphere of 5% CO_2.

Cell viability assay

Cells were seeded in 96-well plates at a density of 8×10^3/well, incubated overnight, and treated with PKWP for 24 h (PKWP group). DMEM instead of PKWP was employed in a control group. MTT (0.5 mg/mL) was added to each well for incubation for 4 h. The formazan crystals formed by live cells were extracted with DMSO, and the absorbance at 490 nm (A) was recorded by a spectrophotometer (MK3, Thermo Fisher Scientific, China). Cell viability was calculated using Eq. 1:

$$\text{Cell viability (\%)} = \frac{\text{PKWP group}}{\text{control group}} \times 100\% \qquad \text{(Eq. 1)}$$

ROS detection

The level of ROS was measured with DCFH-DA. DCFH-DA can penetrate the cell membrane, and be deacetylated to form DCFH, while DCFH can be oxidised by ROS to fluorescent DCF. After being treated with or without PKWP for 24 h, cells were incubated with DCFH-DA (10 μmol/L) at 37°C for 30 min. Then, cells were observed and photographed under laser confocal fluorescence microscopy (LSM800, Zeiss, Germany).

Levels of MDA and GSH, and activities of CAT and T-SOD assay

Cells were seeded into the 6-well plate, left to adhere overnight, and then treated with different concentrations of PKWP for 24 h. The levels of MDA and SGH and activities of CAT and T-SOD were assayed following the kit's instructions.

Western blot analysis

Cells were treated with different concentrations of PKWP for 24 h. The cell lysates were collected, and protein concentration was analysed by BCA Protein Kit. The proteins were first separated by SDS-PAGE (Sodium dodecyl sulphate-

polyacrylamide gel electrophoresis), and then transferred onto the PVDF membrane, followed by blocking with 5% skim milk for 3 h. The membrane was washed thrice with TBST (Tris-buffered saline with Tween 20), and first incubated with the primary antibodies (GAPDH, COX-2, HO-1) (1:1000) at 4°C overnight, and then incubated with secondary antibody (1:2000) at 25°C for 3 h. The bands were visualised with chemiluminescent substrates (Enhanced chemiluminescence (ECL), Engreen Biosystem, Beijing, China), and exposed by a Molecular Imager ChemiDoc XRS System (JS-3000, Bio-Rad, China).

Extraction and derivatisation of cellular metabolites
Extraction of cellular metabolites

Cells were seeded into 100 mm dishes at a density of 3×10^6, and left to adhere overnight, followed by treatment with or without PKWP for 24 h. Then, cells were washed twice with pre-cold PBS, drained thoroughly, and quenched immediately with liquid nitrogen. Cells were collected into a centrifuge tube after addition of 1 mL of pre-chilled extraction reagent (methanol:water = 4:1, v/v, containing 10 μg/mL of internal standard tridecanoic acid), whirled for 1 min, and centrifuged at 4°C for 15 min (15,000 *g*). The supernatant was then gathered and lyophilised for later use.

Derivatisation of cellular metabolites

Each sample was sealed during the derivatisation process to ensure that there was no water throughout the process. The lyophilised samples were mixed with 50 μL of methoxypyridine solution (20 mg/mL), whirled for 1 min, sonicated for 5 min, and then derived at 37°C for 1.5 h. MSTFA was subsequently mixed, followed by derivatisation for 1 h at 37°C. After centrifugation at 4°C for 15 min (13,000 *g*), the supernatant solution was collected for later detection.

Gas chromatography-mass spectrometry (GC-MS) analysis

For chromatographic analysis, HP-5 MS column (30 × 250 × 0.25 μm; J&W Scientific, Folsom, CA) was used. Helium gas was the carrier gas, the linear velocity was 40.0 cm/s, and the split ratio was 10:1. The inlet and transfer line temperature were set at 300 and 250°C. The temperature was programmed at an initial temperature of 70°C (hold for 3 min), and to 300°C as a final temperature at an increasing rate of 5°C/min (hold for 10 min). For GC-MS detection, the solvent cut time was 5.5 min, the energy ionisation was 70 eV, and the ionisation temperature was 230°C. The scanning range was 33 to 600 (*m/z*), and the scan period was 0.2 s. Tentative identification of the compounds was performed by comparing the relative retention time and mass spectra with those of the library data (NIST, Fiehn, Wiley, *etc*.), and then standard samples were applied for further confirmation.

Statistical analysis

SIMCA 14.1 was employed to perform orthogonal partial least squares discriminant analysis (OPLS-DA) and Randomized Permutation test (RPT) on the data, followed by screening and identification analysis of differential metabolites. Student's *t*-test at the univariate level was for the significance of models, and metabolites with the VIP value > 1 and p values < 0.05 were considered statistically significant. The heat map and pathway analysis associated with differential metabolites were generated using MetaboAnalyst 5.0.

Other experimental results were analysed with Origin 2018, Image J, and Statistix 9 software. One-way ANOVA (analysis of variance) was used to compare the sample and the control group. The value of $p < 0.05$ was considered statistically significant.

Results

PKWP inhibited cell viability in concentration-dependent manner

We first evaluated the effect of PKWP on HepG2 cell viability. The results suggested that PKWP significantly inhibited the proliferation of HepG2 cells, as indicated in Figure 1. Compared with the control group, HepG2 cell viability gradually decreased with the increase in PKWP concentration. Cell viability decreased to 87.34 ± 0.42% ($p < 0.01$) after cells were treated with 12.5 μg/mL of PKWP. Cell viability significantly dropped to 84.28 ± 1.32% ($p < 0.01$) with 25.0 μg/mL of PKWP, and further decreased to 54.78 ± 1.26% ($p < 0.01$) with 100.0 μg/mL of PKWP. The number of cells decreased to less than 47.43 ± 0.41% after exposure to 200.0 μg/mL of PKWP. The IC_{50} value of PKWP in HepG2 cells was 106.7 μg/mL (24 h).

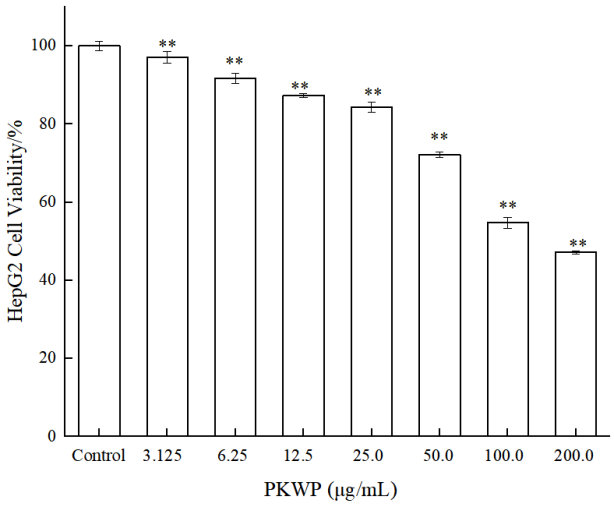

Figure 1. Effect of PKWP on HepG2 cell viability. HepG2 cells were treated with various concentrations of PKWP for 24 h, and cell viability was assayed using MTT. Values are mean ± standard deviation (n = 5). **$p < 0.01$ *vs*. Control.

PKWP altered HepG2 cell metabolism

Cell samples of the control cells without treatment (control group, n = 6) and the cells with PKWP treatment (PKWP group, n = 6) were analysed using a GC-MS-based metabolomics analysis. The OPLS-DA is a supervised discriminant analysis statistical method, and could produce a better separation between classification groups. The OPLS-DA score parameters $R^2X = 0.675$, $Q^2Y = 0.991$, and $Q^2 = 0.969$ (Figure 2A). There was a significant difference between the control and PKWP group in the 95% confidence region, indicating that the model was established successfully. The Permutation test with 100 responses was used to verify the model, showing $R^2 = 0.625$ (Figure 2B). This indicated that the model could effectively explain the differences between two groups of samples, and there was no overfitting. These data showed that the model had highly effective validation and predictability for subsequent analysis. PKWP had a significant regulatory effect on cell metabolism.

Differential metabolites analysis

In the metabolites analysis and volcano plot analysis (Figure 3), we screened 32 differential metabolites with significant changes, which included 11 organic acids, eight amino acids, six saccharides, five alkyl compounds, and three others. Table 1 shows the quantities of some metabolites that have changed. It was suggested that the levels of 11 metabolites were significantly up-regulated, which included putrescine, tyrosine, D-altrose, methionine, pyrophosphate, pantothenic acid, 1-amino cyclopentane formic acid, L-glutamic acid, L-valine, hexamethyldisilane, and isoleucine. The levels of 21 metabolites significantly decreased, which included D-mannopyranose, talose, pyruvic acid, 3,8-dimethyldecane, 3-phosphoglyceric acid, 4-hydroxypyridine, butanedioic acid, D-glucose, citric acid, D-mannose, cysteine, allo-inositol, pentadecanoic acid, D-galactose, 2-methyloctacocane, phosphoenolpyruvic acid (PEP), octamethyltrisiloxane, 4,6-dimethyldodecane, monomethyl phosphate, propanoic acid, and trimethyl-silanophosphate (3:1).

Metabolic pathway enrichment analysis

The data in Figure 4 show that more than ten metabolic pathways were involved, and five metabolic pathways were notably altered, including the tricyclic acid (TCA) cycle, alanine, aspartate and glutamate metabolism, cysteine and methionine metabolism, pyruvate metabolism, and glycolysis/gluconeogenesis. These results indicated that PKWP could regulate various metabolic pathways within HepG2 cells, leading to metabolic disorders.

PKWP triggered oxidative stress in HepG2 cells

The level of ROS is greatly influenced by the cellular redox-controlling system in the body. As shown in Figure 5A, a large amount of ROS was accumulated in PKWP-treated cells, and the level of ROS increased with the increased concentration of PKWP. The intracellular level of ROS in the group treated with 50 μg/mL of PKWP was nearly nine times higher than that of the control group ($p < 0.01$).

As shown in Figure 5B, after PKWP treatment, the content of MDA showed an increasing trend ($p < 0.01$), but only the group with the highest concentration of PKWP showed a significant difference compared to the control group. MDA is the final product of lipid peroxidation, and the results suggested that PKWP could aggravate cell oxidative damage by promoting lipid peroxidation in HepG2 cells.

The results in Figures 5C and 5D suggested that the enzyme activities of T-SOD and CAT, and the level of GSH in HepG2 cells, treated with PKWP significantly decreased in a concentration-dependent manner compared to the control group ($p < 0.01$). The results indicated that PKWP lowered the activities of

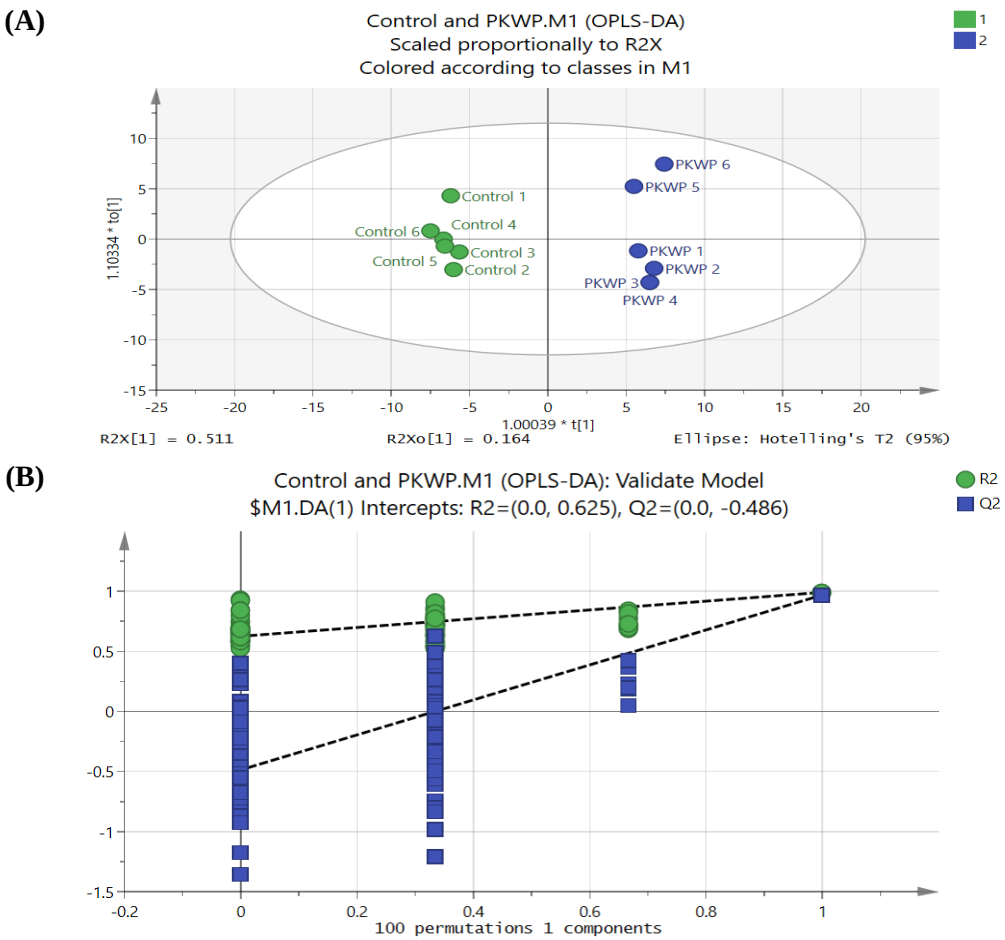

Figure 2. Effect of PKWP on HepG2 cell metabolism. SIMCA 14.1 was applied to perform a principal component analysis of HepG2 cells in Control and PKWP groups. **(A)** Orthogonal partial least squares discriminant analysis (OPLS-DA) score plot. **(B)** The model was validated using a permutation test of 100 responses, and yielded the results of the replacement test.

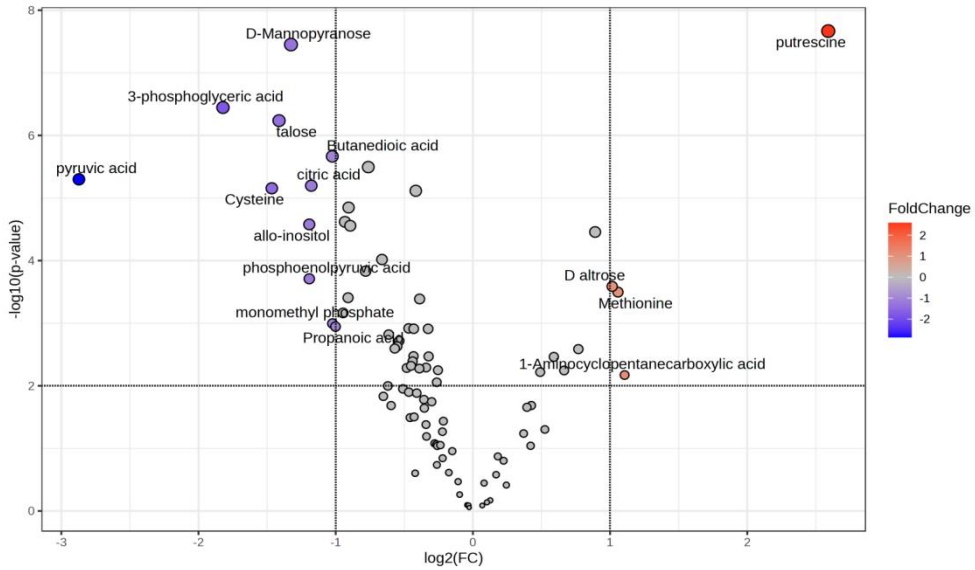

Figure 3. Effect of PKWP on HepG2 cell differential metabolites. Volcano plot analysis of Control and PKWP groups by MetabolicAnalyzer 5.0 ($p < 0.05$, VIP Value > 1, FC Value > 2).

Table 1. Metabolites and relative contents of Control and PKWP groups.

Compound	RT (min)	FC (PKWP/Control)	VIP	$-\log_{10} p$
Putrescine	25.4667	6.0215	1.36915	7.6668
D-Mannopyranose	30.5917	0.39885	1.35941	7.4515
Talose	29.2375	0.37556	1.35805	6.2365
Pyruvic acid	28.2417	0.13663	1.31342	5.2984
3,8-DimethylDecane	19.1083	0.58947	1.33729	5.4944
3-Phosphoglyceric acid	27.1042	0.28288	1.33574	6.4461
4-Hydroxypyridine	10.2833	0.74941	1.33229	5.1154
Butanedioic acid	1.2726	0.49151	1.32011	5.6652
D-Glucose	28.8792	0.52387	1.31363	4.6193
Citric acid	27.3458	0.44194	1.3109	5.197
D-Mannose	28.6583	0.53368	1.30691	4.848
Cysteine	12.4	0.36207	1.30555	5.1556
Tyrosine	28.7125	1.8545	1.30028	4.457
Allo-inositol	32.575	0.43752	1.28776	4.5784
Pentadecanoic acid	30.0458	0.53823	1.28278	4.5567
D-Galactose	29.2458	0.63176	1.2706	4.0175
2-Methyloctacocane	24.7167	0.58162	1.26533	3.8315
D-Altrose	33.4625	2.0213	1.2363	3.5882
Phosphoenolpyruvic acid	22.4583	0.43755	1.23253	4.5567
Methionine	17.7458	2.0815	1.21075	3.4969
Octamethyltrisiloxane	15.2708	0.53225	1.07285	3.4071
4,6-DimethylDodecane	15.1875	0.76399	1.20637	3.3872
Pyrophosphate	23.8625	1.4051	1.03259	2.2191
Monomethyl phosphate	11.1208	0.49195	1.17203	2.9948
Propanoic acid	15.575	0.4995	1.3808	2.9459
1-Aminocyclopentanecarboxylic acid	14.5833	2.1522	1.06231	2.1719
Isoleucine	11.0792	1.3386	1.01755	1.0416
L-Valine	8.2375	1.3143	1.06233	1.6568
L-Glutamic acid	20.5208	1.3436	1.04924	1.6853
Pantothenic acid	40.3042	1.5054	1.09974	2.4624
Hexamethyldisilane	41.1667	1.4385	1.07536	1.3024
Trimethyl-silanophosphate (3:1)	14.0417	0.51904	1.13922	3.1643

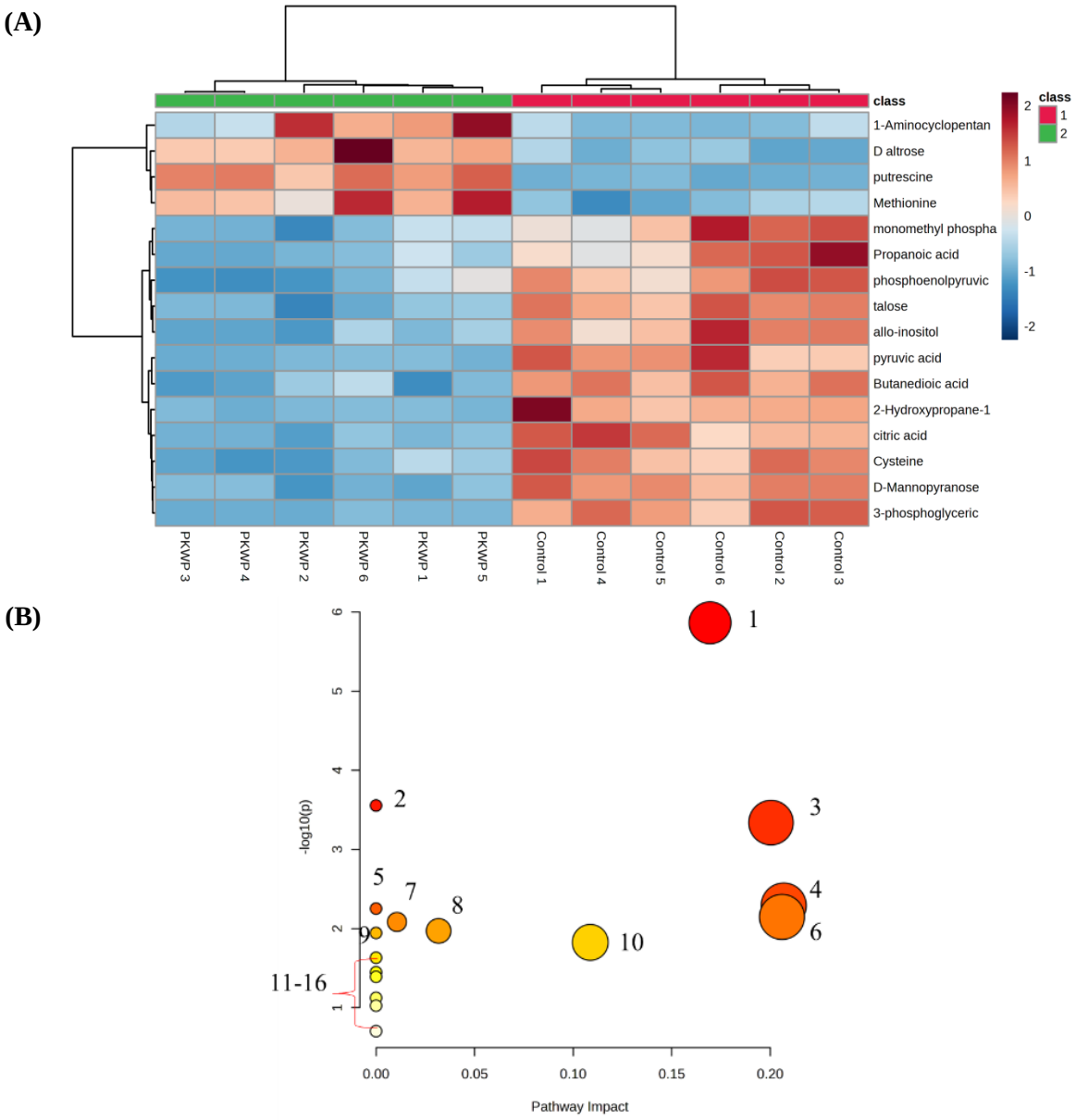

Figure 4. Effect of PKWP on HepG2 cell Biomarker heatmap **(A)** and metabolic pathway **(B)**. Metabolism analysis of HepG2 cells in Control and PKWP groups. Colours shown in Figure 4A are based on FC of metabolites. Red represents high concentrations, and blue represents low concentrations. Horizontal rows represent metabolites, and vertical columns represent samples. In Figure 4B, the larger the -log *p*, the redder the colour, indicating more significance. Radius of the node represents impact of specific metabolic pathway; the larger the radius of the node, the greater the impact. 1: citrate cycle (TCA cycle): 2: alanine, aspartate, and glutamate metabolisms; 3: cysteine and methionine metabolisms; 4: pyruvate metabolism; 5: propanoate metabolism; 6: glycolysis/gluconeogenesis; 7: glutathione metabolism; 8: glyoxylate and dicarboxylate metabolisms; 9: glycine, serine, and threonine metabolisms; 10: arginine and proline metabolisms; 11: aminoacyl-tRNA biosynthesis; 12: thiamine metabolism; 13: taurine and hypotaurine metabolisms; 14: butanoate metabolism; 15: pantothenate and CoA biosyntheses; and 16: tyrosine metabolism.

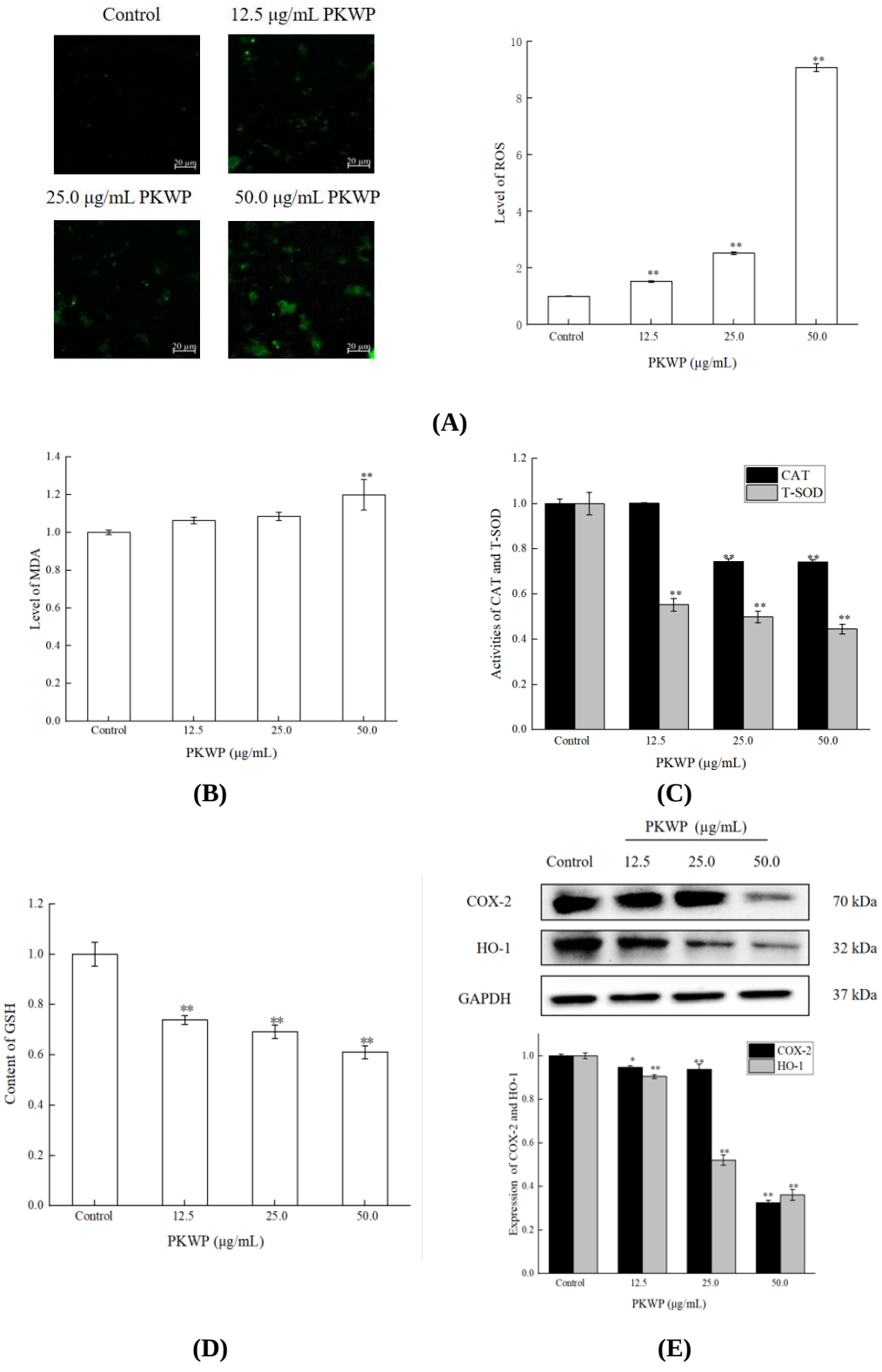

Figure 5. Effect of PKWP on ROS **(A)**, MDA **(B)**, CAT and T-SOD **(C)**, GSH **(D)**, and COX-2 and HO-1 **(E)** of HepG2 cell. Values are mean ± standard deviation ($n = 3$). $^{**}p < 0.01$ *vs*. Control.

T-SOD and CAT, and the level of GSH in HepG2 cells, leading to a decrease in cellular antioxidant capacity.

In the present work, the protein expression of HO-1 and COX-2 significantly decreased after being treated with PKWP for 24 h (Figure 5E). PKWP down-regulated the protein levels of HO-1 and COX-2 in a concentration-dependent manner. The results suggested that PKWP inhibited the expressions of HO-1 and COX-2, potentially weakening their resistance against internal or external stress.

Discussion

Cancer cells generally upregulate their energy production by increasing glycolysis, oxidation of fatty acids or amino acids, but also subsequent TCA cycle and oxidative phosphorylation (OXPHOS), depending on the availability of substrates. Glycolysis represents the most crucial glucose metabolism pathway in cancer cells, and many of its intermediates provide crucial materials for normal metabolism such as oxidative phosphorylation and the TCA cycle. Based on the Warburg theory, cancer cells are characterised by the so-called aerobic glycolysis, in which glycolysis is enhanced even in abundant oxygen, and pyruvate is converted to lactate, although glycolysis is energy-less efficient (Benny *et al*., 2020; Bai *et al*., 2023; Muluh *et al*., 2023). Besides faster glucose consumption, cancer cells have higher capacity to uptake and utilise mannose than normal cells. Mannose can bind to specific receptors on the surface of cancer cells, promoting them to uptake mannose. Talose is a C-2 epimer of galactose. The decreased levels of monosaccharides in the PKWP group indicated that PKWP may inhibit the synthesis of these energy substances. It is known that 3-phosphoglycerate has glycolytic properties and high-energy phosphate bonds. The decrease in the level of 3-phosphoglycerate was also a reflection of the decreased glycolysis ability. Butanedioic acid is a central product of the TCA cycle. Butanedioic acid has antioxidant properties, and promotes energy metabolism. The contents of citric acid and butanedioic acid decreased, indicating that the TCA cycle was inhibited. Propionic acid, an intermediate product, participates in the TCA cycle, and produces ATP through oxidative metabolism. The decreased level of propionic acid also reflected the inhibition of the energy supply chain. Pyruvate is a vital intermediate product in metabolic processes, and it is the hub for the mutual conversion of saccharides, lipids, and proteins. PEP is an intermediate product between glycolysis and gluconeogenesis in cells. In the final step of glycolysis, PEP will be catalysed by pyruvate kinase to produce ATP and pyruvate. During gluconeogenesis, pyruvate must be first converted into oxaloacetate, which would be further catalysed to produce PEP. The decreased levels of pyruvate and PEP suggested the inhibition of pyruvate metabolism.

Amino acids are also major nutrients to produce energy in cancer cells, and cancer cells usually have high amino acid metabolic requirements to accommodate rapid proliferation. Approaches that inhibit the production or utilisation of amino acids may also work effectively as anti-cancer therapies. A high consumption rate of tyrosine and glutamine/glutamate is a common metabolic characteristic of cancer cells. Tyrosine is an amino acid with the function of producing saccharides and ketones. Glutamine/glutamate is the principal energy source for many tumours, and provides macromolecular intermediates for rapid growth and proliferation (Qiu *et al*., 2023). Proliferated tumour cells rely on glutamine to meet the TCA cycle. Isoleucine, leucine, and valine are branched-chain amino acids (BCAAs). The decomposition of branched-chain amino acids (BCAAs) can provide substrates for synthesising other substances. For example, isoleucine and valine can provide carbon precursors to synthesise glucose, and supply fuel for the TCA cycle of cancer cells (Sivanand and Vander Heiden, 2020). Due to growth inhibition, it is unlikely to catabolise a large amount of valine, isoleucine, tyrosine, and glutamate. PKWP may cause stagnation of energy metabolism, and these amino acids could not participate in catabolism, and thus they accumulated. In the liver, alanine releases ammonia through a combined deamination process, and produces pyruvate. The decrease in the level of pyruvate indicated a disorder in the alanine metabolism pathway.

Methionine is an essential amino acid, and a precursor of other substances, such as cysteine, S-adenosyl-L-methionine (SAM), and GSH. The backbone of methionine biosynthesis mainly comes from aspartic acid. Methionine plays a central role in methylation. Methionine must be catalysed by adenosyltransferase to form S-adenosylmethionine (SAM). SAM is catalysed by methyltransferase to

transfer methyl groups to another substance, and generates S-adenosine homocysteine after demethylation. S-adenosine homocysteine is then demethylated to produce homocysteine. Homocysteine undergoes methylation and regenerates methionine, forming the methionine cycle. 1-amino cyclopentane formic acid is a specific inhibitor of SAM-mediated methylation. The increased levels of 1-amino cyclopentane formic acid and methionine implied that methionine utilisation and the methylation cycle were inhibited. Cysteine provides a carbon source for the TCA cycle, and promotes the generation of ATP. Cysteine is also involved in synthesising organic substances such as GSH, 3-mercaptopyruvate, and homocysteine, and mediates tumour proliferation, metastasis, and drug resistance. The contents of cysteine and GSH both decreased after PKWP treatment. These data were consistent with the result of metabolic pathway enrichment (metabolism disorder of cysteine and methionine), and also agreed with the decreased level of GSH.

Putrescine may be a double-edged sword with dose-dependent properties. At low concentrations, it produces significant cell protective and proliferative effects. If excessive, it possibly causes cell inhibition or toxicity. PKWP could cause the accumulation of putrescine, which may induce cell death.

Based on data from the metabolic analysis, PKWP mainly inhibited saccharides synthesis and glycolysis, and reduced gluconeogenesis in HepG2 cells, as indicated by the decreased levels of monosaccharides, citric acid, butanedioic acid, propionic acid, pyruvate, and 3-phosphoglycerate. PKWP also restricted the utilisation of amino acids indicated by inhibiting both the methylation cycle and the catabolism of amino acids, and reducing methionine conversion to cysteine. It is speculated that PKWP might interfere with the amino acid transport system in cells or inhibit various catabolic enzymes. However, further research is needed to verify these speculations.

Several studies suggested that cancers depend on sustained glycolytic metabolism with enhanced antioxidant pathways to modulate redox status (Hess and Khasawneh, 2015; Li *et al*., 2015). Generally speaking, low to moderate levels of ROS are beneficial for maintaining intracellular signalling transduction, whereas high levels of ROS may induce malignant transformation, cell injury, and even death (Malla *et al*., 2021). It has been reported that cancer cells with higher glucose uptake could be used to facilitate the breakdown of ROS. Moreover, it is also assumed that cells may be forced to derive energy from mitochondrial metabolism due to lipid metabolism when restricting glucose metabolism, causing cancer cells to endure OS. Therefore, cancer cells exhibit relatively higher basal levels of ROS than normal cells due to acidic microenvironment modifications, genomic instability, metabolism alterations, and mitochondrial dysfunction (Aki *et al*., 2023). As a consequence, cancer cells carefully and precisely maintain increased steady-state levels of ROS. However, this state of ROS can also be targeted as a vulnerability, as cancer cells are more sensitive to excess ROS. Therefore, manipulating intracellular redox status could be a promising and attractive way for cancer treatment (Slika *et al*., 2022). Enhancing oxidative metabolism by some means simultaneously restrict glucose metabolism, that may cause OS in cancer cells, ultimately resulting in cell death. We found that PKWP not only effectively limited glucose metabolism, but also stimulated OS, as evidenced by the accumulation of ROS and aggravation of lipid peroxidation.

Cells have developed an antioxidant defence system, including exogenous and endogenous antioxidants, and detoxifying enzymes to counteract oxidative damage, and protect cells against injury. Endogenous antioxidants contain antioxidant enzymes, catalytic antioxidant proteins, and small molecular scavengers. T-SOD, CAT, and GSH are crucial components of the intracellular antioxidant system (Pisoschi *et al*., 2021; Rather *et al*., 2021). Cancer cells adapted to OS also demonstrated an up-regulated expression level of HO-1 and COX-2. HO-1 catalyses the oxidative degradation of heme groups, and is highly inducible by various stimuli, such as pro-inflammatory cytokines, ROS, nitric oxide (NO), and ultraviolet irradiation (Loboda *et al*., 2015). The HO-1 pathway has long been regarded as a cytoprotective mechanism against OS. It is proposed that enhanced expression of HO-1 is tumour-promoting, and HO-1 also confers drug resistance to cancer cells. However, some studies have also reported that increased expression of HO-1 stimulates cell death in various types of cancers (Kikuchi *et al*., 2005; Raut and Park, 2020). COX-2 is usually undetectable in normal conditions, but highly inducible and rapidly elevated in response to various inflammatory stimulations. Notably, overexpressed COX-2 participates in multiple stages of cancer

(Toomey *et al*., 2009). Based on epidemiological studies, long-term use of COX-2 inhibitors could lower the incidence and risk of cancers, and improve the efficacy of chemotherapy. Indeed, COX-2 has been recommended as a target for cancer therapy or chemoprevention (Li *et al*., 2020; Halim *et al*., 2023). In the present work, PKWP significantly reduced the expression levels of HO-1 and COX-2, which was consistent with the reduced activities of T-SOD and CAT, as well as the level of GSH. These results suggested that PKWP weakened the antioxidant defence system in HepG2 cells, threatening the survival of cells.

It has been reported that the peels of *Actinidia chinensis* contained higher contents of polyphenols than the flesh, which include isoquercetin, epigallocatechin, catechin, ferulic acid, epicatechin, gallic acid, quercetin, and rutin. Catechin, epicatechin, quercetin, and epigallocatechin are dominant polyphenols (Alim *et al*., 2019). It was also found that peels of green kiwi contained relatively higher level of B-type (epi) catechin dimer, and showed better bioactivity (Dias *et al*., 2020). These polyphenols may be responsible for the remarkable anti-cancer activity of PKWP. However, further in-depth research related to the regulatory activity of each specific polyphenol is still needed to better clarify the anti-cancer mechanism of PKWP.

Conclusion

The present work showed that PKWP exhibited a promising anti-cancer effect. Mechanistically, PKWP caused metabolic disorders by inhibiting saccharide synthesis and glycolysis, reducing gluconeogenesis, and restricting the utilisation of amino acids. PKWP also induced OS by stimulating ROS production, inhibiting expressions of HO-1 and COX-2, and lowering antioxidant enzymes. These results revealed the possible anti-cancer mechanism of PKWP through limiting energy metabolism and triggering oxidative stress, providing evidence for in-depth research and the application of PKWP.

Acknowledgement

The present work was financially supported by the National Natural Science Foundation of China (grant no.: 21707086), the Scientific Research Program Funded by Shaanxi Provincial Education Department (grant no.: 22JK0293), the Xi'an Science and Technology Bureau (grant nos.: 22NYYF048, 21NYYF0022), the Enterprise Cooperation Projects (grant no.: 210210176), the National Foreign Expert Project Funded by the Ministry of Science and Technology of the People's Republic of China (grant no.: G2022041012L), the Shaanxi Provincial Natural Science Foundation (grant no.: 2019JQ-453), the Shaanxi Provincial Department of Science and Technology (grant nos.: 2022NY-035, 2021ZDLNY04-01, 2022ZDLNY04-05), and the Science and Technology Plan of the Weiyang District in Shaanxi Province (grant no.: 202313).

References

Aki, S., Nakahara, R., Maeda, K. and Osawa, T. 2023. Cancer metabolism within tumor microenvironments. Biochimica et Biophysica Acta General Subjects 1867(5): 130330.

Alim, A., Li, T., Nisar, T., Ren, D., Zhai, X., Pang, Y. and Yang, X. 2019. Antioxidant, antimicrobial, and antiproliferative activity-based comparative study of peel and flesh polyphenols from *Actinidia chinensis*. Food and Nutrition Research 26: 29219.

Bai, R., Meng, Y. and Cui, J. 2023. Therapeutic strategies targeting metabolic characteristics of cancer cells. Critical Reviews in Oncology/Hematology 187: 104037.

Benny, S., Mishra, R., Manojkumar, M. K. and Aneesh, T. P. 2020. From Warburg effect to Reverse Warburg effect; the new horizons of anti-cancer therapy. Medical Hypotheses 144: 110216.

Çam, M., İçyer, N. C. and Erdoğan, F. 2014. Pomegranate peel phenolics: Microencapsulation, storage stability and potential ingredient for functional food development. LWT - Food Science and Technology 55(10): 117-123.

Chen, S. N., Liu, X. Y., Zhao, H. A., Cheng, N., Sun, J. and Cao, W. 2022. Beneficial effects of *Gynostemma pentaphyllum* honey paste on obesity *via* counteracting oxidative stress and inflammation: An exploration of functional food developed from two independent foods rich in saponins and phenolics. Food Research International 157: 111483.

Dias, M., Caleja, C., Pereira, C., Calhelha, R. C., Kostic, M., Sokovic, M., ... and Ferreira, I. C. F. R. 2020. Chemical composition and

bioactive properties of byproducts from two different kiwi varieties. Food Research International 127: 108753.

Echave, J., Riaz, Rajoka, M. S., Barba, F. J., Cao, H., Xiao, J., Prieto, M. A. and Simal-Gandara, J. 2021. Valorization of kiwi agricultural waste and industry by-products by recovering bioactive compounds and applications as food additives: A circular economy model. Food Chemistry 15(370): 131315.

Finley, L. W. S. 2023. What is cancer metabolism? Cell 186(8): 1670-1688.

Halim, P. A., Sharkawi, S. M. Z. and Labib, M. B. 2023. Novel pyrazole-based COX-2 inhibitors as potential anticancer agents: Design, synthesis, cytotoxic effect against resistant cancer cells, cell cycle arrest, apoptosis induction and dual EGFR/Topo-1 inhibition. Bioorganic Chemistry 131: 106273.

Hess, J. A. and Khasawneh, M. K. 2015. Cancer metabolism and oxidative stress: Insights into carcinogenesis and chemotherapy *via* the non-dihydrofolate reductase effects of methotrexate. BBA Clinical 3: 152-161.

Jiang, H., Zuo, J., Li, B., Chen, R., Luo, K., Xiang, X., ... and Gao, F. 2023. Drug-induced oxidative stress in cancer treatments: Angel or devil? Redox Biology 63: 102754.

Kikuchi, G., Yoshida, T. and Noguchi, M. 2005. Heme oxygenase and heme degradation. Biochemical and Biophysical Research Communications 338(1): 558-567.

Kroemer, G. and Pouyssegur, J. 2008. Tumor cell metabolism: Cancer's Achilles' heel. Cancer Cell 13(6): 472-482.

Lennicke, C. and Cochemé, H. M. 2021. Redox metabolism: ROS as specific molecular regulators of cell signaling and function. Molecular Cell 81(18): 3691-3707.

Li, L., Fath, M. A., Scarbrough, P. M., Watson, W. H. and Spitz, D. R. 2015. Combined inhibition of glycolysis, the pentose cycle, and thioredoxin metabolism selectively increases cytotoxicity and oxidative stress in human breast and prostate cancer. Redox Biology 4: 127-135.

Li, M., Wu, S., Zhuang, C., Shi, C., Gu, L., Wang, P., ... and Liu, Z. 2022. Metabolomic analysis of circulating tumor cells derived liver metastasis of colorectal cancer. Heliyon 9(1): e12515.

Li, S., Jiang, M., Wang, L. and Yu, S. 2020. Combined chemotherapy with cyclooxygenase-2 (COX-2) inhibitors in treating human cancers: Recent advancement. Biomedicine and Pharmacotherapy 129: 110389.

Li, W., Chen, H., Xu, B., Wang, Y., Zhang, C. Y., Cao, Y. and Xing, X. H. 2023. Research progress on classification, sources and functions of dietary polyphenols for prevention and treatment of chronic diseases. Journal of Future Foods 3(4): 289-305.

Loboda, A., Jozkowicz, A. and Dulak, J. 2015. HO-1/CO system in tumor growth, angiogenesis and metabolism - Targeting HO-1 as an anti-tumor therapy. Vascular Pharmacology 74: 11-22.

Malla, R., Surepalli, N., Farran, B., Malhotra, S. V. and Nagaraju, G. P. 2021. Reactive oxygen species (ROS): Critical roles in breast tumor microenvironment. Critical Review in Oncology/Hematology 160: 103285.

Mukherjee, S., Gupta, P., Ghosh, S., Choudhury, S., Das, A., Ahir, M., ... and Chattopadhyay, S. 2023. Targeted tumor killing by pomegranate polyphenols: Pro-oxidant role of a classical antioxidant. The Journal of Nutritional Biochemistry 115: 109283.

Muluh, T. A., Shu, X. S. and Ying, Y. 2023. Targeting cancer metabolic vulnerabilities for advanced therapeutic efficacy. Biomed and Pharmacotherapy 162: 114658.

Pang, H. H. and Hu, Z. P. 2023. Metabolomics in drug research and development: The recent advances in technologies and applications. Acta Pharmacologica Sinica B 13(8): 3238-3251.

Pisoschi, A. M., Pop, A., Iordache, F., Stanca, L., Predoi, G. and Serban, A. I. 2021. Oxidative stress mitigation by antioxidants - An overview on their chemistry and influences on health status. European Journal of Medical Chemistry 209: 112891.

Qian, X., Zhu, L., Xu, M., Liu, H., Yu, X., Shao, Q. and Qin, J. 2023. Shikonin suppresses small cell lung cancer growth *via* inducing ATF3-mediated ferroptosis to promote ROS accumulation. Chemico-Biological Interactions 382: 110588.

Qiu, H., Shao, N., Liu, J., Zhao, J., Chen, C., Li, Q., ... and Xu, L. 2023. Amino acid metabolism in tumor: New shine in the fog? Clinical Nutrition 42: 1521-1530.

Rather, G. M., Pramono, A. A., Szekely, Z., Bertino, J. R. and Tedeschi, P. M. 2021. In cancer, all roads lead to NADPH. Pharmacology and Therapeutics 226: 107864.

Raut, P. K. and Park, P. H. 2020. Globular adiponectin antagonizes leptin-induced growth of cancer cells by modulating inflammasomes activation: Critical role of HO-1 signaling. Biochemical Pharmacology 180: 114186.

Rotariu, D., Babes, E. E., Tit, D. M, Moisi, M., Bustea, C., Stoicescu, M., … and Bungau, S. G. 2022. Oxidative stress - Complex pathological issues concerning the hallmark of cardiovascular and metabolic disorders. Biomedicine and Pharmacotherapy 152: 113238.

Rumgay, H., Arnold, M., Ferlay, J., Lesi, O., Cabasag, C. J., Vignat, J., … and Soerjomataram, I. 2022. Global burden of primary liver cancer in 2020 and predictions to 2040. Journal of Hepatology 77(6): 1598-1606.

Sanati, M., Afshari, A. R., Kesharwani, P., Sukhorukov, V. N. and Sahebkar, A. 2022. Recent trends in the application of nanoparticles in cancer therapy: The involvement of oxidative stress. Journal of Controlled Release 348: 287-304.

Sanz, V., López-Hortas, L., Torres, M.-D. and Domínguez, H. 2021. Trends in kiwifruit and byproducts valorization. Trends in Food Science and Technology 107: 401-414.

Sivanand, S. and Vander Heiden, M. G. 2020. Emerging roles for branched-chain amino acid metabolism in cancer. Cancer Cell 37(2): 147-156.

Slika, H., Mansour, H., Wehbe, N., Nasser, S. A., Iratni, R., Nasrallah, G., ... and Eid, A. H. 2022. Therapeutic potential of flavonoids in cancer: ROS-mediated mechanisms. Biomedicine and Pharmacotherapy 146: 112442.

Toomey, D. P., Murphy, J. F. and Conlon, K. C. 2009. COX-2, VEGF and tumor angiogenesis. The Surgeon 7(3): 174-180.

Tuy, K., Rickenbacker, L. and Hjelmeland, A. B. 2021. Reactive oxygen species produced by altered tumor metabolism impacts cancer stem cell maintenance. Redox Biology 44: 101953.

Wang, S., Qiu, Y. and Zhu, F. 2021. Kiwifruit (*Actinidia* spp.): A review of chemical diversity and biological activities. Food Chemistry 350: 128469.

Yuan, J., Khan, S. U., Yan, J., Lu, J., Yang, C. and Tong, Q. 2023. Baicalin enhances the efficacy of 5-Fluorouracil in gastric cancer by promoting ROS-mediated ferroptosis. Biomedicine and Pharmacotherapy 164: 114986.

Zhong, Y. C., Cheng, J. W., Wang, P. X., Fan, J., Zhou, J. and Yang, X. R. 2023. Opportunities and challenges of liquid biopsy in liver cancer. Clinical Surgical Oncology 2(4): 100026.

Zhou, X., An, B., Lin, Y., Ni, Y., Zhao, X. and Liang, X. 2023. Molecular mechanisms of ROS-modulated cancer chemoresistance and therapeutic strategies. Biomedicine and Pharmacotherapy 165: 115036.